A Modular System for the Synthesis of Multiplexed Magnetic Resonance Probes

6 AUTHORS, INCLUDING:

Victoria S R Harrison
Northwestern University
6 PUBLICATIONS **81** CITATIONS

SEE PROFILE

Amanda L Eckermann
Hope College
28 PUBLICATIONS **598** CITATIONS

SEE PROFILE

Claudio Luchinat
University of Florence
609 PUBLICATIONS **14,478** CITATIONS

SEE PROFILE

# A Modular System for the Synthesis of Multiplexed Magnetic Resonance Probes

Daniel J. Mastarone,[†] Victoria S. R. Harrison,[†] Amanda L. Eckermann,[†] Giacomo Parigi,[‡] Claudio Luchinat,[‡] and Thomas J. Meade*,[†]

[†]Department of Chemistry, Molecular Biosciences, Neurobiology and Physiology, and Radiology, Northwestern University, 2145 Sheridan Road, Evanston, Illinois 60208-3113, United States

[‡]CERM and Department of Chemistry, University of Florence, via L. Sacconi 6, 50019 Sesto Florence, Italy

ⓢ Supporting Information

ABSTRACT: We have developed a modular architecture for preparing high-relaxivity multiplexed probes utilizing click chemistry. Our system incorporates azide bearing Gd(III) chelates and a trialkyne scaffold with a functional group for subsequent modification. In optimizing the relaxivity of this new complex, we undertook a study of the linker length between a chelate and the scaffold to determine its effect on relaxivity. The results show a strong dependence on flexibility between the individual chelates and the scaffold with decreasing linker length leading to significant increases in relaxivity. Nuclear magnetic resonance dispersion (NMRD) spectra were obtained to confirm a 10-fold increase in the rotational correlation time from 0.049 to 0.60 ns at 310 K. We have additionally obtained a crystal structure demonstrating that modification with an azide does not impact the coordination of the lanthanide. The resulting multinuclear center has a 500% increase in per Gd (or ionic) relaxivity at 1.41 T versus small molecule contrast agents and a 170% increase in relaxivity at 9.4 T.
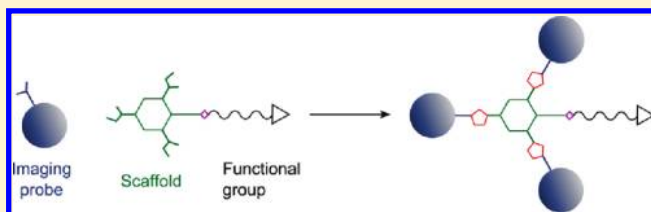
■ INTRODUCTION

Magnetic resonance imaging (MRI) is a widely used modality in experimental research and clinical diagnostics.[2] The intrinsic contrast of MR images can be augmented by the use of MR contrast agents (CAs) that are derived from two primary classes: superparamagnetic particles[3−5] and paramagnetic chelates.[6] The relaxivity ($mM^{-1} s^{-1}$) of a paramagnetic contrast agent reflects its ability to shorten the T_1 relaxation time of water which results in a brighter MR image. The higher the relaxivity, the more sensitive the agent.[6,7]

During the past decade, there has been a surge in the development of new gadolinium-based MR contrast agents. These efforts have focused on signal amplification, targeting, and bioactivated or responsive probes.[7−22] Recently, multimodal agents have emerged that enhance MR contrast and simultaneously provide the ability to image the target with other techniques (fluorescence microscopy or positron emission tomography)[12,23] for in vivo targeting and fate mapping of cells.[8,22]

The relaxivity of MR contrast agents depends heavily on magnetic field strength.[24] At low magnetic fields (1.5−3 T), the relaxivity of small molecule contrast agents are limited by their short rotational correlation time (τ_R).[7] As shown in eq 1 an optimal relaxivity occurs when the correlation time (τ_{c1}) of the Gd(III) CA is equal to the inverse of the Larmor frequency ($1/\omega_I$) of the proton. This correlation time contains contributions from three process, τ_R the rotational correlation time, τ_m the mean water residence lifetime, and T_{1e} the electronic relaxation time. By attaching a small molecule CA to a macromolecule (e.g., protein, polymer, nanoparticle, viral capsid), the molecular tumbling decreases resulting in a longer τ_R and a subsequent increases in relaxivity.[7,25−32] Although macromolecular systems have shown significant promise as high relaxivity CAs at low field, they are difficult to characterize and are frequently polydisperse.[31,33] For macromolecular CAs, an increase in relaxivity is observed between 0.5 and 1.5 T due to the field dependence of T_{1e}. The increase in relaxivity is due to the T_{1e} contribution to τ_{c1} resulting from the long τ_R of the macromolecular CAs. However, this increase is followed by a rapid decrease in relaxivity as the field strength increases beyond 1.5 T. This effect results from the long τ_{c1} value which shifts the onset of the relaxation dispersion to smaller proton Larmor frequencies.[34]

$$\tau_{c1}^{opt} = \frac{1}{\omega_I}; \quad \frac{1}{\tau_{c1}} = \frac{1}{\tau_R} + \frac{1}{\tau_m} + \frac{1}{T_{1e}} \qquad (1)$$

The need for increased sensitivity for molecular and cellular imaging in research laboratories has driven the development of high field MR systems.[24,35] Caravan and co-workers demonstrated that as field strength increases the optimal value for τ_R decreases, from ≈20 ns for low field to ≈0.5 ns for high field magnets.[24]

ACS Publications   © 2011 American Chemical Society

5329

dx.doi.org/10.1021/ja1099616 | *J. Am. Chem. Soc.* 2011, 133, 5329–5337

Scheme 1. Synthesis of Contrast Agent 3, from the Trialkyne Core 2, and Gd(III) Contrast Agent 1 through Click Chemistry
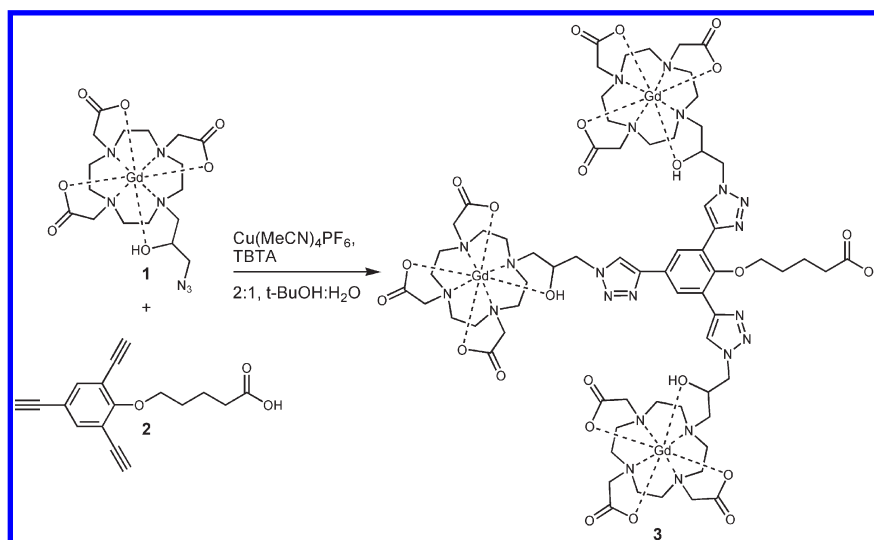
To address the need for contrast agents that can operate effectively in the high field MR instruments and simultaneously provide the option to install multiple modalities, the development of a synthetically flexible contrast agent core is required. Toward this goal, we have designed a new class of contrast agent conjugates that are modular, monodisperse, exhibit high relaxivity, and can be subsequently modified (Scheme 1).

■ RESULTS AND DISCUSSION

Several examples of multimeric conjugates with *intermediate* τ_R values between (0.5 and 4 ns) exist in the literature.[22,36] For example, the work of Martin and co-workers is an early example of a modular agent that has been modified with a fatty acid to bind to bovine serum albumin (BSA).[37] Ranganathan and co-workers have found a 25% increase in relaxivity when the number of freely rotating atoms in their linker was decreased.[38] Additionally, a 40% increase in relaxivity was seen by Henig and co-workers in their silsesquioxane contrast agents by changing from an ethylene to a benzene linker.[39] The multimeric complexes of Livramento and Kotková demonstrate very high relaxivities at 20 and 60 MHz due to increased size and hydration number.[40−43] These last two examples have shown promise as high field agents but do not possess further functionality for targeted or multimodal imaging projects. The properties of these agents are compared in Table 1. In related work with macromolecular agents, Zhang and Nair use peptide tetramers designed to bind to human serum albumin (HSA) or fibrin and demonstrate that multilocus binding results in an increase in relaxivity due to increased rigidity.[44−46] Avedano and Datta show that increasing the rigidity of their linkers (alkyl vs aromatic) to HSA and viral capsids respectively increased relaxivity by more than 50%.[29,47] The works of Rudovsky and co-workers demonstrate the importance of internal motion in dendritic systems by utilizing ion paring between the PAMAM dendrimer and a polyarginine to reduce internal motion and increase relaxivity.[48,49]

We have previously demonstrated that the triazole linkages formed by click chemistry are effective in generating multimeric CAs with relatively high relaxivities as a result of increased linker

rigidity.[22] Here, we describe three new azide-functionalized chelates and a new phenol-based scaffold with three alkyne groups to take advantage of facile click chemistry. The alcohol functional group on the phenol scaffold is orthogonal to click chemistry and can be used in subsequent modification.

The new macrocyclic chelates **1**, **4**, and **5** were designed to investigate the effect of linker length on relaxivity (Figure 1). Preparation begins with a ring-opening of epichlorohydrin with sodium azide to provide 1-azido-3-chloropropan-2-ol **6**. Addition of **6** to the trisubstituted macrocycle (tris-*t*-butyl-DO3A) provides the protected ligand **7**. Deprotection of the *t*-butyl esters with formic acid at 50 °C followed by metalation provides contrast agent **1** after HPLC purification (Scheme 2). Chelates **4** and **5** were prepared from tris-*t*-butyl-DO3A-monoacetic acid and $N_3(CH_2)_nNH_2$ through peptide coupling where $n = 2, 3$ see (Scheme 1, Supporting Information). These chelates were metalated using $Gd(OAc)_3$ and purified using reverse phase HPLC.

Complex **1** was characterized by X-ray crystallographic analysis (v:v:v, 1:1:1, mixture of water, acetonitrile, and acetone) and revealed no significant differences between the chelate structure of **1** and $[Gd(HP\text{-}DO3A)(H_2O)]$ (Figure 2).[50] The O8−Gd bond length is consistent with that reported for $[Gd(HP\text{-}DO3A)(H_2O)]$ (ProHance) indicating that the overall structure is not perturbed by the addition of the azide at C16 and the coordination geometry of **1** is similar to $[Gd(HP\text{-}DO3A)(H_2O)]$.

Preparation of scaffold **2** is shown in Scheme 3. The synthesis begins with the alkylation of tribromophenol with ethyl 5-bromovalerate in DMF with K_2CO_3 overnight at 50 °C to form **8** in high yield. A Sonogashira reaction using **8** and trimethylsilyl (TMS) acetylene provides the protected trialkyne **9**. The TMS groups are removed using KF in ethanol and the ethyl ester is saponified in dioxane/water with NaOH to form the desired scaffold **2** (Scheme 3). This scaffold includes a carboxylic acid that can be functionalized before or after the click chemistry to form the final conjugate.

A series of agents (**3**, **11**, **12**) were synthesized with 1, 3, or 4 methylene groups between the scaffold and the chelate. Click

Table 1. Summary of Multimeric Contrast Agents[a]

ref	field strength MHz	solution	temperature °C	q	per gd relaxivity mM^{-1} s^{-1}	no. of Gd(III) centers	molecular relaxivity mM^{-1} s^{-1}
this work[b]	60	DPBS	37	1	15.4	3	46.2
this work[b]	60	water	37	1	8.9	3	26.7
this work[b]	60	water	37	1	7.3	3	21.9
Zhang[b]	64	TBS	35	1	12.5	4	50
Zhang[b]	64	TBS/fibrin	35	1	18	4	72
Song	60	water	37	1	5.9	3	17.7
Song	60	water	37	1	11	6	65.8
Song	60	water	37	1	12.2	7	85.4
Gd(HP-DO3A)	60	MOPS	37	1	3	1	3
Jebasingh	24	Tris pH 5.6	35	2	7	4	28.1
Zhang[b]	20	PBS	37	1	10.3	4	41.2
Zhang[b]	20	PBS/HSA	37	1	39.1	4	156.4
Nair[b]	20	TBS	37	1	20.6	4	82.4
Nair[b]	20	TBS/fibrin	37	1	27.7	4	110.8
Martin[b]	20	water	N/A	1	10.4	4	41.6
Martin[b]	20	water/BSA	N/A	1	24.6	4	98.4
Martin[b]	20	water	N/A	1	4.7	2	9.4
Martin[b]	20	water/BSA	N/A	1	9.3	2	18.6
Kotková[c]	20	water	25	1	21.6	6.9	149
Livramento	20	water	37	2	15.7	3	47.1
Livramento	20	water	37	2	20.1	6	120.6
Ranganathan	20	water	40	1	13.0	8	104
Ranganathan	20	water	40	1	9.8	4	39.2
Ranganathan	20	water	40	1	5.4	2	10.8
Henig	20	water	25	1	12.1	8	96.8
Henig	20	water	25	1	17.1	8	136.8
Gd(DTPA)	20	water	N/A	1	4.5	1	4.5

[a] The contrast agents in this table are divided based on the field strength of relaxivity measurements. The differences in field strengths and temperature used in collecting this relaxivity data make it difficult to compare to the molecules in our current work. In general relaxivity decreases from 20 to 60 MHz, and relaxivity also decreases with increasing temperature. [b] Bifunctional. [c] Multimodal.
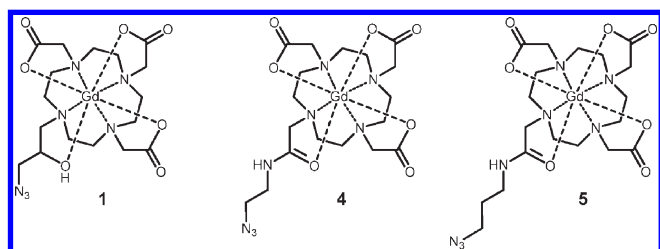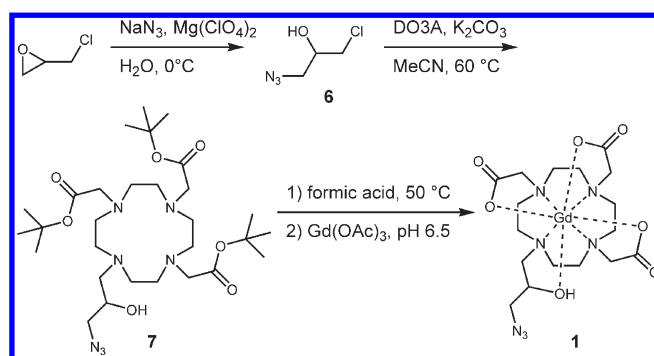

Figure 1. Macrocyclic chelates with increasing linker length.

Scheme 2. Synthesis of Complex 1

chemistry was used to conjugate **1**, **4**, and **5** to scaffold **2** using standard conditions resulting in an observable correlation between relaxivity and linker length. The longest linker (**12**) has the lowest relaxivity (7.3 mM^{-1} s^{-1} at 1.41 T), while the shortest linker (**3**) exhibits the highest relaxivity (15.4 mM^{-1} s^{-1} at 1.41 T) (Figure 3). This result is not surprising considering that increasing the rigidity of the linker between the scaffold and the individual chelates limits local rotation. This effect has been shown to increase relaxivity in other systems.[22,26,38] It should be noted that τ_m could be an additional limitation to the relaxivity of (**11**) and (**12**) due to the monoamide ligand structure of these chelates.

[Eu(HPN$_3$DO3A)(H$_2$O)] was synthesized to confirm that the addition of the azide to the structure did not perturb the

hydration number q in solution. Fluorescence analysis of [Eu(HPN$_3$DO3A)(H$_2$O)] showed a value of 0.90 ± 0.1. Following attachment of [Eu(HPN$_3$DO3A)(H$_2$O)] to scaffold **2** the hydration number was maintained at 0.87 ± 0.1. These results confirm that the addition of the azide and the subsequent click chemistry do not affect the hydration number. The relaxivities of **1** and **3** were measured at 1.41 T and **1** is similar to [Gd(HP-DO3A)(H$_2$O)] (Table 2). At this low field strength, the per Gd relaxivity of **3** is 5-fold higher than that of **1**.
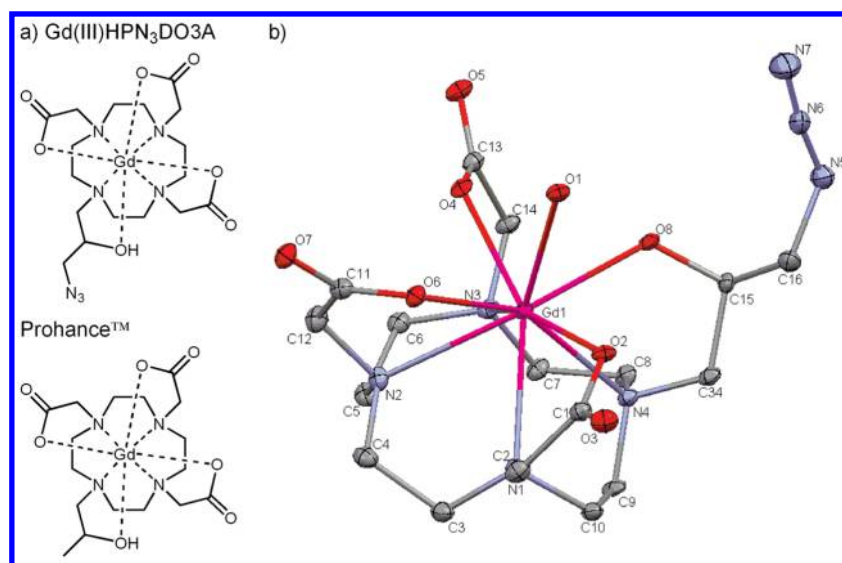
Figure 2. (a) 2D structures of $[Gd(HPN_3DO3A)(H_2O)]$ (**1**) and $[Gd(HPDO3A)(H_2O)]$ (b) Thermal ellipsoid plot of (**1**) drawn at 35% probability level. Hydrogen atoms are omitted for clarity. Distances (Å): Gd1−O1 = 2.47; Gd1−O2 = 2.37; Gd1−O8 = 2.43. The differences between these values and the corresponding values for $[Gd(HP-DO3A)(H_2O)]$ are 0.03, 0.01, 0.01, respectively.

Scheme 3. Alkyne Scaffold 2 Designed for Orthogonal Modification through Click Chemistry with 1 and Peptide Coupling
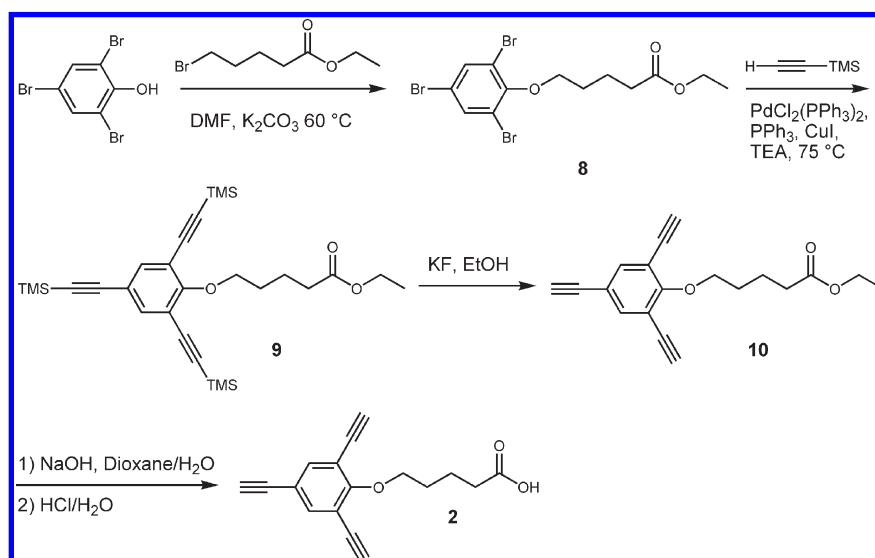
To observe the effect of field strength on the relaxivities of **1** and **3**, these values were measured at 9.4 T. At this field strength, the relaxivity of **1** is only 10% lower than at 1.41 T, while **3** shows a 70% decrease. This effect is typical of small molecule chelates such as **1** with short τ_R values. In these cases, the relaxation rates are relatively unaffected by field strength. The pronounced decrease in relaxivity of **3** at higher field strength suggests the complex has a long τ_R. The per Gd relaxivity of **3** at 9.4 T is 170% that of **1**. By controlling the size of the CA, τ_R can be regulated to achieve a significant increase in relaxivity.

To obtain a better estimate of the increase in the τ_R between compounds **1** and **3**, water proton relaxivity was measured from 0.01 to 40 MHz proton Larmor frequency (corresponding to fields of 0.0002−0.95 T) for **1** and **3** at 298 and 310 K (Figure 4). The nuclear magnetic resonance dispersion (NMRD) profiles[35] of **1** exhibit a single dispersion. This result is ascribed to one water molecule coordinated to the paramagnetic Gd(III) ion, the protons of which are dipolarly coupled to the electron spins with a correlation time corresponding to the tumbling time of a small molecule, and the additional contribution of diffusing water molecules. The relaxivity of **3** is (i) much larger than that of **1** and (ii) exhibits a dispersion occurring at smaller frequencies. Both features indicate that the correlation time τ_{c1} is sizably increased.[51] A peak in relaxivity appears in the high frequency region, indicating that the correlation time is field dependent and must be affected by the electron relaxation time T_{1e}. In turn, this result means that for **3**, τ_R is longer than T_{1e} at least
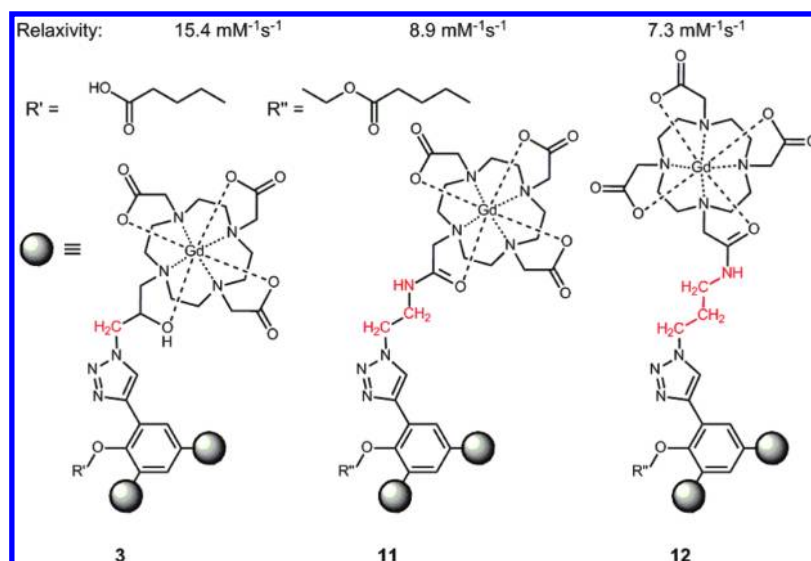
Figure 3. As the linker length between the azide and the chelate increases (left to right) the relaxivities (at 1.41 T and 310 K) decrease. This effect is attributed to a reduction in the local rotation of the chelates for the shorter linker lengths.

Table 2. Relaxivities of Compounds 1 and 3 at 1.41 and 9.4 T at 37 °C

field	1.41 T		9.4 T	
	per Gd(III)	molecular	per Gd(III)	molecular
[Gd(HP-DO3A)(H$_2$O)]	2.99 ± 0.5^a	2.99 ± 05^a		
1 (mM^{-1} s^{-1})	3.05 ± 0.06^b	3.05 ± 0.06^b	2.79 ± 0.04^b	2.79 ± 0.04^b
3 (mM^{-1} s^{-1})	15.4 ± 0.8^b	46.2 ± 2.4^b	4.8 ± 0.3^b	14.4 ± 0.9^b

^{a} 10 mM MOPS, 100 mM NaCl, pH 7.4, 37 °C.[1] ^{b} DPBS 10 mM, pH 7.4, 37 °C.

at low fields, so that at such fields T_{1e} dominates the correlation time τ_{c1}. T_{1e} increases with increasing magnetic field strength, and therefore the correlation time τ_{c1} is determined by both τ_R and T_{1e} in the high field region of Figure 4. The temperature dependence observed in the relaxivity profiles of both complexes indicates that water molecules are in the fast exchange regime. Therefore, their τ_m is not strongly limiting the relaxivity.

The profiles for **1** have been fit (solid lines in Figure 4) using the standard Solomon-Bloembergen-Morgan (SMB) model,[52,53] that is, neglecting the presence of static zero-field splitting (ZFS), and the Freed equation.[54,55] These models calculate the inner-sphere and the outer-sphere contributions, respectively. The SBM model describes the relaxation profiles from the number of coordinated water molecules and their distance from the unpaired electrons, and from several dynamic parameters, that are the molecular reorientation time, the electron relaxation time, and the lifetime of coordinated water protons. The Freed equation describes the contribution to relaxation due to water molecules freely diffusing around the paramagnetic complex through the diffusion constant, the distance of closest approach, and the electron relaxation time. We assume that the two protons of the coordinated water molecule are located at 3.1 Å from the metal ion, with lifetimes τ_m of 350 and 300 ns at 298 and 310 K respectively, as previously found for [Gd(HP-DO3A)(H$_2$O)] at 298 K.[56] Diffusion water molecules were considered with standard values for the diffusion constants of 2.5×10^{-5} and 3.5×10^{-5} cm^2 s^{-1} at 298 and 310 K,[51] respectively, and a distance of closest approach of 3.6 Å. The best fit parameters were the
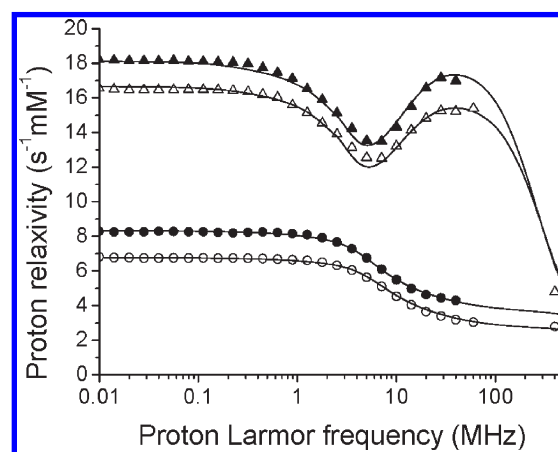

Figure 4. Water proton relaxativity data for complexes **1** (●, ○) and **3** (▲, △) at 298 K (solid symbols) and 310 K (open symbols). The solid lines are the best-fit curves (see text).

field-dependent electron relaxation time, T_{1e}, described by the transient ZFS Δ_t and the electron correlation time τ_v, and the tumbling time τ_R. The calculated best fit values were 0.027 ± 0.003 cm^{-1} for Δ_t, 28 ± 2 and 26 ± 3 ps for τ_v at 298 and 310 K, respectively, and 0.067 ± 0.004 and 0.049 ± 0.004 ns for τ_R at 298 and 310 K, respectively. These values correspond well to those previously obtained for similar small Gd(III) complexes by analyzing the relaxation data using the same model.[6]

5333

dx.doi.org/10.1021/ja1099616 |*J. Am. Chem. Soc.* 2011, 133, 5329–5337

Table 3. Rotational Correlation Times of Compounds 1 and 3 at 298 and 310 K

	τ_R	
	298 K	310 K
1	0.067 ± 0.004 ns[a]	0.049 ± 0.004 ns[a]
3	0.74 ± 0.03 ns[a]	0.60 ± 0.02 ns[a]

[a] Gd(III) proton distance 3.1 Å, τ_M of 350 and 300 ns at 298 and 310 K, diffusion rate of water 2.5×10^5 and 3.5×10^5 cm^{2}s^{-1} at 298 and 310 K.

The profiles for **3** could not be satisfactorily fit using the SBM model presumably due to the effect of a static ZFS in the presence of a slower molecular tumbling. The profiles were fit according to the "modified Florence" approach[53,57−59] to obtain estimates of the parameters on which the relaxivity depends. In such an approach, the effect of static ZFS on the splitting of the energy levels of all spin states is considered for the calculation of the nuclear spectral densities, provided that τ_R is much larger than T_{1e}. The solid lines in Figure 4 are the best-fit curves obtained for the two protons of the coordinated water molecule at 3.1 Å from the metal ion with a τ_R of 0.74 ± 0.03 ns and of 0.60 ± 0.02 ns at 298 and 310 K, respectively. All other parameters have the same values used in the analysis performed with the SBM and Freed models, except for the transient ZFS Δ_t of 0.018 ± 0.001 cm^{-1}, τ_v of 23 ± 2 ps, and the static ZFS of 0.024 ± 0.005 cm^{-1}. Figure 4 shows that higher field data are in reasonably good agreement with the best-fit profiles obtained from relaxation data measured up to 40 MHz.

The overall agreement between the calculated curves and the experimental data shows that the main features of all profiles can be reproduced as the result of an increase in τ_R upon conjugation of **1** to **3**. (Table 3) The change in the values of electron relaxation parameters between **1** to **3** (similar to that observed for other gadolinium complexes when bound to macromolecules)[27,60,61] is likely determined by the simultaneous presence of both static and transient ZFS, which is not fully accounted for in fast rotating systems by available fitting programs.[53,62] Both profiles of **1** and **3** were fit according to the "modified Florence" approach, and the main features of all profiles could be reproduced as the result of an increase in τ_R on passing from **1** to **3** (see Supporting Information, Figure S1). Independent from the electronic parameters, the analysis clearly shows that the NMRD profiles of **3** can only be reproduced for tumbling times that are approximately 1 order of magnitude larger than those of **1**.

Conjugation of **1** to **3** results in an increase in τ_R from 0.049 to 0.60 ns at 310 K resulting in a 2-fold increase in relaxivity at low field and a 5-fold increase at the peak value of 40 MHz. The analysis of the data is consistent with an essentially unaltered hydration of the Gd(III) complex upon conjugation to the scaffold and shows that the increase of relaxivity is due to the increase in τ_R. The 10-fold increase in τ_R upon the conjugation of **1** to **3** places the molecule in the *intermediate* τ_R range between (0.5 and 4 ns). This range has been predicted to be optimal for imaging at higher magnet field strengths.[24]

MR images were obtained of complexes **1** and **3** in glass capillaries (1 mm) at 7 T (Figure 5). Molecular concentrations ranged from 60 to 7.5 μM. The image was obtained using a RARE pulse sequence with a TE and TR of 11 and 200 ms. Not surprisingly, **3** is clearly brighter than **1** at the same molecular
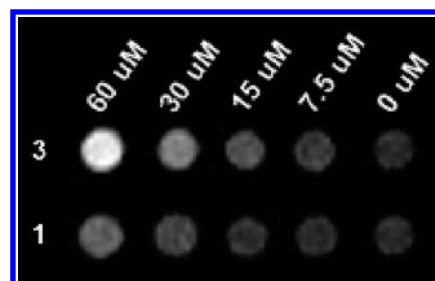

Figure 5. MR images of **3** and **1** at 7 T using a RARE pulse sequence with a TE/TR of 11/200 ms. The molecular concentrations of **3** and **1** range from 60 μM to 7.5 μM in 10 mM DPBS. The Gd(III) ionic concentration is three times higher for compound **3** than for **1** based on the molecular structure.

concentration. This data demonstrate the improved performance of **3** vs **1** at high field strength which results in significant contrast enhancement.

In conclusion, we have developed a multiplexed and modular MR contrast agent scaffold with a 500% increase in per Gd relaxivity at 1.41 T and a 170% increase at 9.4 T versus small molecule MR agents. Using this approach, we are preparing scaffolds that support multiple CAs while simultaneously providing the ability to incorporate functional groups for subsequent modification with targeting ligands, fluorophores, and nanoparticles.

■ EXPERIMENTAL SECTION

General Synthetic Methods. Unless noted, materials and solvents were purchased from Sigma-Aldrich Chemical Co. (St. Louis, MO) and used without further purification. GdCl$_3$·6H$_2$O and 1,4,7,10-tetraazacyclododecane (cyclen) were purchased from Strem Chemicals (Newburyport, MA) and used without further purification. Unless noted, all reactions were performed under a nitrogen atmosphere. THF, acetonitrile, and dichloromethane were purified using a Glass Contour Solvent system. Deionized water was obtained from a Millipore Q-Guard System equipped with a quantum Ex cartridge (Billerica, MA). Thin-layer chromatography (TLC) was performed on EMD 60F 254 silca gel plates. Visualization of compounds was accomplished using either an iodoplatinate or UV light. Standard grade 60 Å 230−400 mesh silca gel (Sorbent Technologies) was used for flash column chromatography.

^{1}H and ^{13}C NMR spectra were obtained on a Bruker 500 MHz Avance III NMR Spectrometer or a Varian Inova 400 MHz NMR spectrometer with deuterated solvent as noted. Electrospray ionization mass spectrometry (ESI-MS) spectra were taken on a Varian 1200 L single-quadrupole mass spectrometer. High resolution mass spectrometry data was aquired on an Agilent 6210 LC-TOF (ESI, APCI, APPI). Analytical reverse-phase HPLC-MS was performed on a Varian Prostar 500 system with a Waters 4.6×250 mm 5 μM Atlantis C18 column. This system is equipped with a Varian 380 LC ELSD system, a Varian 363 fluorescence detector, and a Varian 335 UV−vis detector. Preparative runs were performed on a Water 19×250 mm Atlantis C18 Column. The mobile phases consisted of Millipore water (A) and HPLC-grade acetonitrile (B). HPLC method 1: 0−5 min 100% A, 5−24:08 min 57.5% A, 24:08−30 min 0% A, 30−35 min 0% A, 35−40 min 100% A.

Determination of r_1 was accomplished using a Bruker minispec 60 MHz (1.41 T) magnet and a Varian Inova 400 MHz (9.4 T) NMR spectrometer. At 1.41 T, the T_1 relaxation times were determined using an inversion recovery method, while at 9.4 T a saturation recovery

5334

dx.doi.org/10.1021/ja1099616 |*J. Am. Chem. Soc.* 2011, 133, 5329–5337

method was used. The saturation recovery method utilized a 2 s presaturation pulse centered on the water frequency. All measurements were done at 37 °C at an approximate 1 mM concentration of CA in 10 mM DPBS purchased from Invitrogen.

NMRD measurements were performed with a Stelar Spinmaster FFC-2000-1T fast field cycling relaxometer in the 0.01−40 MHz proton Larmor frequency range at 298 and 310 K. Standard field cycling protocol was used. Longitudinal water proton relaxation rates were obtained with an error smaller than 1%. Proton nuclear magnetic relaxation dispersion (NMRD) profiles were obtained by plotting proton relaxation rates as a function of applied magnetic field after subtraction of the diamagnetic contribution of buffer alone and normalization to 1 mM Gd(III) concentration.

1-Azido-3-chloropropan-2-ol (6) . **6** was synthesized as described by Ingham et al with the following modifications.[63] Diethyl ether was used in the place of dichloromethane in the procedure. The final product was not distilled as in the literature procedure but simply extracted into ether and evaporated. The product was used directly in subsequent reactions. *Caution:* Safe handling procedures for perchlorates and small molecule azides should be reviewed before performing this reaction, as there is a danger of explosion if heat, friction, or shock is applied.

Tritert-butyl 2,2′,2′′-(1,4,7,10-tetraazacyclododecane-1, 4,7-triyl)triacetate hydrobromide (tris-t-butyl-DO3A HBr). Tris-t-butyl-DO3A HBr was synthesized according to the procedure of Oskar with the following modifications.[64] To a 500 mL RB flask was added 10.279 g (59.8 mmol) of cyclen to which was added 14.8405 g (179.2 mmol) of NaOAc. The solids were dissolved in 180 mL of dimethylacetamide (DMA). The reaction was cooled to 0 °C with ice and 26.5 mL (179.3 mmol) of *tert*-butyl bromoacetate dissolved in 70 mL of DMA was added dropwise over 40 min at 0 °C. The reaction was allowed to warm to RT and stirred for two days and was poured into a solution of 16.6 g of KBr in 1000 mL of H_2O. The solution was brought to a basic pH with 17.7 g (3.5 equiv) of $NaHCO_3$. (*Caution*: A large amount of gas is produced.) A total of 10 mL of ether was added to initiate precipitation of the HBr salt of tris-t-butyl-DO3A. The final white to off white powder was filtered and dried under a vacuum to give a yield of 21.4976 g (60% yield). ^{1}H NMR (500 MHz, $CDCl_3$) δ 3.56−2.57 (m, 21H), 1.46 (d, J = 3.6 Hz, 27H). ^{13}C NMR (126 MHz, $CDCl_3$) δ 170.53, 169.63, 81.86, 81.71, 77.29, 77.04, 76.78, 58.22, 51.31, 51.12, 49.14, 47.53, 28.23, 28.19, 28.03, 0.00.

Tritert-butyl 2,2′,2′′-(10-(3-azido-2-hydroxypropyl)-1,4,7, 10-tetraazacyclododecane-1,4,7-triyl)triacetate (7). To a 250 mL round-bottom was added 4.9963 g (8.397 mmol) of tris-t-butyl-DO3A and 2.8957 g (20.98 mmol) of K_2CO_3. The flask was charged with 80 mL of anhydrous acetonitrile. The flask was sealed and placed under a nitrogen atmosphere. 1.6957 g (12.50 mmol) of **6** was dissolved in 5 mL of acetonitrile and added to the solution of tris-t-butyl-DO3A. The reaction was heated to 50 °C and stirred overnight. The reaction was monitored by mass spectrometry to follow the disappearance of the starting materials. 0.399 g (2.94 mmol) of **6** was added and allowed to stir for another 24 h. The reaction was checked by MS to determine the disappearance of tris-t-butyl-DO3A. Once all of the tris-t-butyl-DO3A had disappeared, the reaction was filtered and evaporated to provide a yellow oil. The oil was dissolved in minimal methanol and 100 mL of diethyl ether was added and the flask was placed at −20 °C overnight. 3.968 g (77% yield) of clear to yellow crystals of 7 formed overnight in the freezer and were filtered and washed with cold ether. M/Z observed: 614.5, calculated: 614.4 $[M + H]^+$.

1-(3-Azido-2-hydroxypropyl)-4,7,10-tris(carboxymethyl)-1,4,7,10-tetraazacyclododecyl-gadolinium(III)(1). 1.0201 g (1.661 mmol) (7) was dissolved in 100 mL of formic acid and heated overnight. MS was used to observe the removal of the t-butyl

protecting groups; once complete the formic acid was evaporated on a rotary evaporator. The resulting oil was redissolved in water 3 × 10 mL and evaporated to remove most of the formic acid. The resulting glassy solid was dissolved in 30 mL of water and Gd(OAc)$_3$·6H$_2$O was added. The pH was adjusted to ∼6.5 with 1 M NaOH and the reaction was heated to 50 °C. The pH was adjusted back to 6.5 every 6−10 h until no further change occurred (typically 1−2 days). The reaction was evaporated and purified by reverse phase HPLC according to method 1, retention time of 15.5 min, and 99.9% purity, followed by lyophilization to yield 412 mg of **1** as a white powder in 41% yield based on the starting mass of tris-t-butyl-DO3A. M/Z observed: 597.13151, calculated: 597.13367 $[M + H]^+$.

Ethyl 5-(2,4,6-tribromophenoxy)pentanoate (8). To a 100 mL round-bottom flask was added 970.4 mg (2.933 mmol) of tribromophenol, 483.1 mg (3.500 mmol) of K_2CO_3, and 0.5 mL (3.120 mmol) of ethyl 5-bromovalerate. The flask was charged with 30 mL of dry DMF and nitrogen gas was bubbled through the reaction for 5 min. The reaction was left under nitrogen and brought to 50 °C and stirred for 12 h. Once the reaction was shown to be complete by TLC (9:1 Hex: EtOAc) the reaction was diluted with 50 mL of H_2O and extracted three times with 50 mL of diethyl ether. Afterward, the combined organic layers were dried over $MgSO_4$, filtered, and concentrated using a rotary evaporator. The residue was purified by column chromatography (9:1 hexane: ethyl acetate) to give 1181.8 mg of a yellow to clear oil (88% yield). ^{1}H NMR (500 MHz, $CDCl_3$) δ 7.62 (s, 2H), 4.12 (q, J = 7.1 Hz, 2H), 3.97 (t, J = 5.8 Hz, 2H), 2.40 (t, J = 4.6 Hz, 2H), 1.88 (dt, J = 6.5, 3.2 Hz, 4H), 1.24 (t, J = 7.1 Hz, 3H). ^{13}C NMR (126 MHz, $CDCl_3$) δ 173.70, 153.04, 135.21, 119.27, 117.49, 73.13, 60.54, 34.17, 29.55, 21.66, 14.48. M/Z observed: 456.8653, calculated: 456.8644 $[M+H]^+$.

Ethyl 5-(2,4,6-tris((trimethylsilyl)ethynyl)phenoxy)-pentanoate (9). To a flame-dried 50 mL round-bottom flask was added 0.5793 g (1.265 mmol) of **S-8**, 29.3 mg (0.154 mmol) of copper(I) iodide, and 107.2 mg (0.4092 mmol) of triphenylphosphine. The flask was charged with 12 mL of dry triethylamine. Nitrogen was bubbled through the solution for 5 min followed by the addition of 1.8 mL (13 mmol) of TMS-acetylene and 90.4 mg (0.128 mmol) of bis(triphenylphosphine) palladium-(II) chloride were added. The flask was heated to 75 °C and left to stir overnight under nitrogen. The reaction was concentrated using a rotary evaporator. Thirty milliters of hexane was added to the flask and the remaining solids were filtered off. The hexane solution was concentrated using a rotary evaporator and the final residue was purified by silica gel chromatography (40:1 hexane/ethyl acetate). 606.7 mg of clear oil was obtained (93.8% yield). ^{1}H NMR (500 MHz, $CDCl_3$) δ 7.46 (s, 2H), 4.21 (t, J = 5.9 Hz, 2H), 4.10 (d, J = 7.1 Hz, 2H), 2.37 (t, J = 7.2 Hz, 2H), 1.93−1.73 (m, 4H), 1.23 (t, J = 7.1 Hz, 3H), 0.27 − 0.13 (m, 27H). ^{13}C NMR (126 MHz, $CDCl_3$) δ 173.66, 161.79, 137.59, 118.55, 117.80, 103.10, 100.05, 99.86, 94.69, 73.70, 60.46, 34.27, 29.96, 21.87, 14.46, 0.08, 0.01. M/Z observed: 511.2505, calculated: 511.2515 $[M + H]^+$.

Ethyl 5-(2,4,6-triethynylphenoxy)pentanoate (10). To a 100 mL RB flask was added 214 mg (0.418 mmol) of **S-9** which was dissolved in 20 mL of ethanol. To this was added 366 mg (6.29 mmol) of KF and stirred for 4 h or until the reaction is complete by TLC (19:1 hexanes/ethyl acetate). Once complete the reaction was evaporated and the solids were washed with hexanes. The crude product was purified by column chromatography using 19:1 hexanes/ethyl acetate to provide 116 mg of a colorless to yellow oil in 94% yield. ^{1}H NMR (499 MHz, $CDCl_3$) δ 7.53 (s, 2H), 4.23 (t, J = 5.9 Hz, 2H), 4.11 (q, J = 7.1 Hz, 2H), 3.26 (s, 2H), 3.01 (s, 1H), 2.37 (t, J = 7.2 Hz, 2H), 1.96 − 1.73 (m, 4H), 1.23 (t, J = 7.1 Hz, 3H). ^{13}C NMR (126 MHz, $CDCl_3$) δ 173.74, 162.57, 138.31, 117.76, 117.21, 82.72, 81.55, 78.72, 77.95, 74.05, 60.46, 34.18, 29.75, 21.69, 14.47, 14.40. M/Z observed: 295.1322, calculated: 295.1329 $[M + H]^+$.

5-(2,4,6-Triethynylphenoxy)pentanoic acid (2). 105 mg (0.375 mmol) of **S-10** was dissolved in 5 mL of 1,4 dioxane. To this

5335

dx.doi.org/10.1021/ja1099616 |*J. Am. Chem. Soc.* 2011, 133, 5329–5337

was added 1 mL of 1 M NaOH and the mixture was stirred for 4 h or until completion. 9:1 hexanes/ethyl acetate was indicated by TLC. Five milliliters of water was added to the reaction and the dioxane was evaporated on a rotary evaporator. The remaining water was further diluted by 5 mL of water and acidified with 3 M HCl. Upon reaching an acidic pH, the product precipitated as yellow to orange crystals 86 mg, 91% yield. ^{1}H NMR (499 MHz, CDCl$_3$) δ 7.56 (s, 2H), 4.26 (t, J = 5.9 Hz, 2H), 3.29 (s, 1H), 3.04 (s, 1H), 2.48 (t, J = 7.3 Hz, 2H), 2.01−1.80 (m, 4H). ^{13}C NMR (126 MHz, CDCl$_3$) δ 178.25, 162.27, 138.12, 117.61, 116.99, 82.55, 81.30, 78.47, 77.78, 73.72, 33.37, 29.41, 21.24. M/Z observed: 265.0865, calculated: 265.087 $[M - H]^-$.

General Procedure for Click Chemistry. All click chemistry reactions were done in a 2:1 mixture of t-butanol and water. Compounds **1**, **4**, and **5** (3.3 equiv) were dissolved in the water and compound **2** (1 equiv) was dissolved in t-butanol. The solution of the Gd(III) complex in water was added to the solution of **2** in t-butanol. This solution was bubbled with nitrogen to remove any adventitious oxygen followed by the addition of $[Cu(MeCN)_4]PF_6$ (0.02 equiv) and tris[(1-benzyl-1H-1,2,3-triazol-4-yl)methyl]amine (TBTA) (0.02 equiv). The reaction was left under a nitrogen atmosphere and heated to 50 °C overnight. The reaction was checked by MALDI or HPLC to determine completeness of the reaction. The solvent was removed by lyophilization and the products **3**, **6**, and **7** were purified by reverse phase HPLC utilizing method 1.

*5-(2,4,6-Tris(1-(2-hydroxy-3-(1H-1,2,3-triazol-1-yl)propyl)-4,7,10-tris(carboxymethyl)-1,4,7,10-tetraazacyclododecylgadolinium(**III**))phenoxy)pentanoic acid (**3**).* Purified by HPLC according to method 1, retention time of 17.1 min, and 99.1% purity, M/Z found: 1045.76034, calculated: 1045.76040 $[M + 2H]^{2+}$.

*Ethyl 5-(2,4,6-tris(1-(2-((2-(1H-1,2,3-triazol-1-yl)ethyl)amino)-2-oxoethyl)-4,7,10-tris(carboxymethyl)-1,4,7,10-tetraazacyclododecylgadolinium(**III**))phenoxy)pentanoate (**11**).* Purified by HPLC according to method 1, retention time of 18.6 min, and 99.2% purity, M/Z found: 1085.2790, calculated: 1085.2787 $[M + 2H]^{2+}$.

*Ethyl 5-(2,4,6-tris(1-(2-((2-(1H-1,2,3-triazol-1-yl)propyl)amino)-2-oxoethyl)-4,7,10-tris(carboxymethyl)-1,4,7,10-tetraazacyclododecylgadolinium(**III**))phenoxy)pentanoate (**12**).* Purified by HPLC according to method 1, retention time of 19.1 min, and 98.3% purity, M/Z found: 1105.79946, calculated: 1105.80178 $[M + 2H]^{2+}$.

ASSOCIATED CONTENT

ⓢ Supporting Information. The experimental section (PDF) and X-ray crystallographic files (CIF) material are available free of charge via the Internet at http://pubs.acs.org.

AUTHOR INFORMATION

Corresponding Author
tmeade@northwestern.edu

ACKNOWLEDGMENT

REFERENCES

(1) Duimstra, J. A.; Femia, F. J.; Meade, T. J. *J. Am. Chem. Soc.* **2005**, *127*, 12847.

(2) Modo, M. M., Bulte, J. W. W., Eds.; *Molecular and Cellular MR Imaging*; CRC Press: Boca Raton, FL, 2007.

(3) Laurent, S.; Forge, D.; Port, M.; Roch, A.; Robic, C.; Vander Elst, L.; Muller, R. N. *Chem. Rev.* **2008**, *108*, 2064.

(4) Hu, F.; MacRenaris, K. W.; A. Waters, E.; Schultz-Sikma, E. A.; Eckermann, A. L.; Meade, T. J. *Chem. Commun.* **2010**, *46*, 73.

(5) Hu, F.; MacRenaris, K. W.; Waters, E. A.; Liang, T.; Schultz-Sikma, E. A.; Eckermann, A. L.; Meade, T. J. *J. Phys. Chem. C* **2009**, *113*, 20855.

(6) Caravan, P.; Ellison, J. J.; McMurry, T. J.; Lauffer, R. B. *Chem. Rev.* **1999**, *99*, 2293.

(7) Caravan, P. *Chem. Soc. Rev.* **2006**, *35*, 512.

(8) Major, J. L.; Meade, T. J. *Acc. Chem. Res.* **2009**, *42*, 893.

(9) De Leon-Rodriguez, L. M.; Lubag, A. J. M.; Malloy, C. R.; Martinez, G. V.; Gillies, R. J.; Sherry, A. D. *Acc. Chem. Res.* **2009**, *42*, 948.

(10) Ali, M. M.; Liu, G.; Shah, T.; Flask, C. A.; Pagel, M. D. *Acc. Chem. Res.* **2009**, *42*, 915.

(11) Que, E. L.; Chang, C. J. *J. Am. Chem. Soc.* **2006**, *128*, 15942.

(12) Frullano, L.; Meade, T. J. *J. Biol. Inorg. Chem.* **2007**, *12*, 939.

(13) Meade, T. J.; Aime, S. *Acc. Chem. Res.* **2009**, *42*, 821.

(14) Aime, S.; Castelli, D. D.; Crich, S. G.; Gianolio, E.; Terreno, E. *Acc. Chem. Res.* **2009**, *42*, 822.

(15) Major, J. L.; Boiteau, R. M.; Meade, T. J. *Inorg. Chem.* **2008**, *47*, 10788.

(16) Major, J. L.; Parigi, G.; Luchinat, C.; Meade, T. J. *Proc. Natl. Acad. Sci. U.S.A.* **2007**, *104*, 13881.

(17) Li, W. H.; Fraser, S. E.; Meade, T. J. *J. Am. Chem. Soc.* **1999**, *121*, 1413.

(18) Li, W. H.; Parigi, G.; Fragai, M.; Luchinat, C.; Meade, T. J. *Inorg. Chem.* **2002**, *41*, 4018.

(19) Louie, A. Y.; Huber, M. M.; Ahrens, E. T.; Rothbacher, U.; Moats, R.; Jacobs, R. E.; Fraser, S. E.; Meade, T. J. *Nat. Biotechnol.* **2000**, *18*, 321.

(20) Urbanczyk-Pearson, L. M.; Femia, F. J.; Smith, J.; Parigi, G.; Duimstra, J. A.; Eckermann, A. L.; Luchinat, C.; Meade, T. J. *Inorg. Chem.* **2008**, *47*, 56.

(21) Que, E. L.; Domaille, D. W.; Chang, C. J. *Chem. Rev.* **2008**, *108*, 1517.

(22) Song, Y.; Kohlmeir, E. K.; Meade, T. J. *J. Am. Chem. Soc.* **2008**, *130*, 6662.

(23) Mulder, W. J. M.; Strijkers, G. J.; van Tilborg, G. A. F.; Cormode, D. P.; Fayad, Z. A.; Nicolay, K. *Acc. Chem. Res.* **2009**, *42*, 904.

(24) Caravan, P.; Farrar, C. T.; Frullano, L.; Uppal, R. *Contrast Media Mol. Imaging* **2009**, *4*, 89.

(25) Langereis, S.; Lussanet, Q. G. d.; Genderen, M. H. P. v.; Backes, W. H.; Meijer, E. W. *Macromolecules* **2004**, *37*, 3084.

(26) Nicolle, G. M.; Toth, E.; Schmitt-Willich, H.; Raduechel, B.; Merbach, A. E. *Chem.—Eur. J.* **2002**, *8*, 1040.

(27) Caravan, P.; Parigi, G.; Chasse, J. M.; Cloutier, N. J.; Ellison, J. J.; Lauffer, R. B.; Luchinat, C.; McDermid, S. A.; Spiller, M.; McMurry, T. J. *Inorg. Chem.* **2007**, *46*, 6632.

(28) Endres, P. J.; Paunesku, T.; Vogt, S.; Meade, T. J.; Woloschak, G. E. *J. Am. Chem. Soc.* **2007**, *129*, 15760.

(29) Datta, A.; Hooker, J. M.; Botta, M.; Francis, M. B.; Aime, S.; Raymond, K. N. *J. Am. Chem. Soc.* **2008**, *130*, 2546.

(30) Caravan, P. *Acc. Chem. Res.* **2009**, *42*, 851.

(31) Karfeld-Sulzer, L. S.; Waters, E. A.; Davis, N. E.; Meade, T. J.; Barron, A. E. *Biomacromolecules* **2010**, *11*, 1429.

(32) Manus, L. M.; Mastarone, D. J.; Waters, E. A.; Zhang, X.-Q.; Schultz-Sikma, E. A.; MacRenaris, K. W.; Ho, D.; Meade, T. J. *Nano Lett.* **2009**, *10*, 484.

(33) Weinmann, H.-J.; Ebert, W.; Misselwitz, B.; Schmitt-Willich, H. *Eur. J. Radiol.* **2003**, *46*, 33.

(34) Hermann, P.; Kotek, J.; Kubicek, V.; Lukes, I. *Dalton Trans.* **2008**, 3027.

(35) Merbach, A. E.; Toth, E. *The Chemistry of Contrast Agents in Medical Magnetic Resonance Imaging*Wiley: New York, 2001.

(36) Jebasingh, B.; Alexander, V. *Inorg. Chem.* **2005**, *44*, 9434.

(37) Martin, V. V.; Ralston, W. H.; Hynes, M. R.; Keana, J. F. W. *Bioconjugate Chem.* **1995**, *6*, 616.

(38) Ranganathan, R. S.; Fernandez, M. E.; Kang, S. I.; Nunn, A. D.; Ratsep, P. C.; Pillai, K. M. R.; Zhang, X.; Tweedle, M. F. *Invest. Radiol.* **1998**, *33*, 779.

(39) Henig, J. r.; Tóth, E. v.; Engelmann, J. r.; Gottschalk, S.; Mayer, H. A. *Inorg. Chem.* **2010**, *49*, 6124.

(40) Livramento, J. B.; Helm, L.; Sour, A.; O'Neil, C.; Merbach, A. E.; Toth, E. *Dalton Trans.* **2008**, 1195.

(41) Kotková, Z.; Kotek, J.; Jirák, D.; Jendelová, P.; Herynek, V.; Berková, Z.; Hermann, P.; Lukeš, I. *Chem.—Eur. J.* **2010**, *16*, 10094.

(42) Livramento, J. B.; Sour, A.; Borel, A.; Merbach, A. E.; Tóth, É. *Chem.—Eur. J.* **2006**, *12*, 989.

(43) Livramento, J. B.; Weidensteiner, C.; Prata, M. I. M.; Allegrini, P. R.; Geraldes, C. F. G. C.; Helm, L.; Kneuer, R.; Merbach, A. E.; Santos, A. C.; Schmidt, P.; É, T. *Contrast Media Mol. Imaging* **2006**, *1*, 30.

(44) Nair, S. A.; Kolodziej, A. F.; Bhole, G.; Greenfield, M. T.; McMurry, T. J.; Caravan, P. *Angew. Chem., Int. Ed.* **2008**, *47*, 4918.

(45) Zhang, Z.; Greenfield, M. T.; Spiller, M.; McMurry, T. J.; Lauffer, R. B.; Caravan, P. *Angew. Chem., Int. Ed.* **2005**, *44*, 6766.

(46) Zhang, Z.; Kolodziej, A. F.; Qi, J.; Nair, S. A.; Wang, X; Case, A. W.; Greenfield, M. T.; Graham, P. B.; McMurry, T. J.; Caravan, P. *New J. Chem.* **2010**, *34*, 611.

(47) Avedano, S.; Tei, L.; Lombardi, A.; Giovenzana, G. B.; Aime, S.; Longo, D.; Botta, M. *Chem. Commun.* **2007**, 4726.

(48) Rudovský, J.; Botta, M.; Hermann, P.; Hardcastle, K. I.; Lukeš, I.; Aime, S. *Bioconjugate Chem.* **2006**, *17*, 975.

(49) Rudovsky, J.; Hermann, P.; Botta, M.; Aime, S.; Lukes, I. *Chem. Commun.* **2005**, 2390.

(50) Kumar, K.; Chang, C. A.; Francesconi, L. C.; Dischino, D. D.; Malley, M. F.; Gougoutas, J. Z.; Tweedle, M. F. *Inorg. Chem.* **2002**, *33*, 3567.

(51) Bertini, I.; Luchinat, C.; Parigi, G. *Adv. Inorg. Chem.* **2005**, *57*, 105.

(52) Solomon, I. *Phys. Rev.* **1955**, *99*, 559.

(53) Kowalewski, J.; Kruk, D.; Parigi, G. *Adv. Inorg. Chem.* **2005**, *57*, 41.

(54) Hwang, L.-P.; Freed, J. H. *J. Chem. Phys.* **1975**, *63*, 4017.

(55) Polnaszek, C. F.; Bryant, R. G. *J. Chem. Phys.* **1984**, *81*, 4038.

(56) Aime, S.; Botta, M.; Fasano, M.; Terreno, E. *Acc. Chem. Res.* **1999**, *32*, 941.

(57) Bertini, I.; Galas, O.; Luchinat, C.; Parigi, G. *J. Magn. Reson., Ser A* **1995**, *113*, 151.

(58) Bertini, I.; Kowalewski, J.; Luchinat, C.; Nilsson, T.; Parigi, G. *J. Chem. Phys.* **1999**, *111*, 5795.

(59) Kruk, D.; Nilsson, T.; Kowalewski, J. *Phys. Chem. Chem. Phys.* **2001**, *3*, 4907.

(60) Alhaique, F.; Bertini, I.; Fragai, M.; Carafa, M.; Luchinat, C.; Parigi, G. *Inorg. Chim. Acta* **2002**, *331*, 151.

(61) Bligh, S. A.; Chowdhury, A. H.; Kennedy, D.; Luchinat, C.; Parigi, G. *Magn. Reson. Med.* **1999**, *41*, 767.

(62) Kowalewski, J.; Luchinat, C.; Nilsson, T.; Parigi, G. *J. Phys. Chem. A* **2002**, *106*, 7376.

(63) Ingham, J. D.; Petty, W. L.; Nichols, J. P. L. *J. Org. Chem.* **1956**, *21*, 373.

(64) Oskar, A.; Andreas, O., GE Healthcare AS., WO2006 112723, 2006